Kinetic MHD simulation of nonlinear tearing with large Δ'

Scott E. Parker, Jianhua Cheng, Yang Chen, Dmitri Uzdensky

University of Colorado-Boulder

Outline

- Model equations
- Second order semi-implicit method
- Tearing mode results
  - Linear
  - Nonlinear

Ion equations of motion and field equations

- Lorentz force ions

$$\frac{d\boldsymbol{v}_i}{dt} = \frac{q_i}{m_i}(\boldsymbol{E} + \boldsymbol{v}_i \times \boldsymbol{B})$$
$$\frac{d\boldsymbol{x}_i}{dt} = \boldsymbol{v}_i$$

- Ampere's equation

$$\bigtriangledown \times \boldsymbol{B} = \mu_0 \left(n_i q_i \boldsymbol{u}_i - n_e e \boldsymbol{u}_e \right)$$

- Faraday's law

$$\bigtriangledown \times \boldsymbol{E} = -\frac{\partial \boldsymbol{B}}{\partial t}$$

Generalized Ohm's law

- Using quasi-neutrality $n_i = n_e$, the electron density and flow can be calculated directly from particle ions

$$
\begin{aligned}
& en_i(1+\frac{m_e}{m_i}\frac{q_i^2}{e^2})\boldsymbol{E}+\frac{m_e}{\mu_0 e}\bigtriangledown\times(\bigtriangledown\times\boldsymbol{E}) \\
= & -(1+\frac{m_e}{m_i}\frac{q_i}{e})\,\boldsymbol{j}_i\times\boldsymbol{B}+\frac{1}{\mu_0}(\bigtriangledown\times\boldsymbol{B})\times\boldsymbol{B} \\
& +\eta\frac{en_i}{\mu_0}(1+\frac{m_e}{m_i}\frac{q_i^2}{e^2})\bigtriangledown\times\boldsymbol{B}-\nabla\cdot\boldsymbol{\Pi}_e+\frac{m_e}{m_i}\frac{q_i}{e}\bigtriangledown\cdot\boldsymbol{\Pi}_i,
\end{aligned}
$$

- In general, we need an electron model to calculate Π_e. Here we assume the electrons are isothermal and Π_e reduces to

$$P_e = n_e T_e = n_i T_e$$

Future plans include drift-kinetic and gyro-kinetic electron models.

Second order semi-implicit scheme

- The velocity, length and time are normalized to $c_s^2 = T_e/m_i$, $\rho_s = m_i c_s/eB_0$ and $\Omega_{ci}^{-1} = m_i/eB_0$. $\beta_e = \mu_0 n_0 T_e/B_0^2$ is defined upon the uniform background plasma.
- The equations of motion are

$$\frac{\boldsymbol{x}^{n+1} - \boldsymbol{x}^n}{\Delta t} = (1-\theta)\ \boldsymbol{v}^n + \theta\ \boldsymbol{v}^{n+1},$$
$$\frac{\boldsymbol{v}^{n+1} - \boldsymbol{v}^n}{\Delta t} = (1-\theta)\ \boldsymbol{a}^n + \theta\ \boldsymbol{a}^{n+1},$$
$$\frac{w^{n+1} - w^n}{\Delta t} = -(1-\theta)\ (\boldsymbol{v}^n \cdot \bigtriangledown + \boldsymbol{a}^n \cdot \partial_{\boldsymbol{v}}) \ln f_0(\boldsymbol{x}^n, \boldsymbol{v}^n)$$
$$-\theta\ (\boldsymbol{v}^{n+1} \cdot \bigtriangledown + \boldsymbol{a}^{n+1} \cdot \partial_{\boldsymbol{v}}) \ln f_0(\boldsymbol{x}^{n+1}, \boldsymbol{v}^{n+1}),$$

  where $\boldsymbol{a} = \frac{q_i}{m_i}(\boldsymbol{E} + \boldsymbol{v} \times \boldsymbol{B})$.
- Generalized Ohm's law:

$$(n_{i0} + \delta n_i^{n+1})(1 + \frac{m_e}{m_i} q_i^2)\boldsymbol{E}^{n+1} + \frac{m_e}{m_i}\frac{1}{\beta_e} \bigtriangledown \times(\bigtriangledown \times \boldsymbol{E}^{n+1})$$
$$= -(1 + \frac{m_e}{m_i} q_i)\delta \boldsymbol{j}_i^{n+1} \times (\boldsymbol{B}_0 + \delta \boldsymbol{B}^{n+1}) + \frac{1}{\beta_e}(\bigtriangledown \times \delta \boldsymbol{B}^{n+1}) \times \boldsymbol{B}_0$$
$$+\frac{1}{\beta_e}(\bigtriangledown \times (\boldsymbol{B}_0 + \delta \boldsymbol{B}^{n+1})) \times \delta \boldsymbol{B}^{n+1} + \frac{\eta}{\beta_e}(1 + \frac{m_e}{m_i} q_i^2)(n_{i0} + \delta n_i^{n+1}) \bigtriangledown \times \delta \boldsymbol{B}^{n+1}$$
$$-\nabla \delta n_i^{n+1} + \frac{m_e}{m_i} q_i\ \bigtriangledown \cdot P_i^{n+1},$$

Ion current and nonlinear terms

- The first term on the right hand side of the generalized Ohm's law involves the future ion current density

$$en_i(1+\frac{m_e}{m_i}\frac{q_i^2}{e^2})\boldsymbol{E}^{n+1}+\cdots=-(1+\frac{m_e}{m_i}\frac{q_i}{e})\ \delta\boldsymbol{j}_i^{n+1}\times\boldsymbol{B}^{n+1}+\cdots$$

we approximate $\delta\boldsymbol{j}_i^{n+1}$ as follows

$$\begin{aligned}\delta\boldsymbol{j}_i^{n+1}&=q_i\ \sum_j w_j^{n+1}\boldsymbol{v}_j^{n+1}\\&=\delta\boldsymbol{j}_i^{\star}+q_i\ \theta\ \Delta t\ \sum_j\frac{q_i}{T_i}\boldsymbol{E}^{n+1}(\boldsymbol{x}_j^{n+1})\cdot\boldsymbol{v}_j^{n+1}\boldsymbol{v}_j^{n+1}\\&\simeq\delta\boldsymbol{j}_i^{\star}+\theta\ \Delta t\ \frac{q_i^2}{m_i}\ \boldsymbol{E}^{n+1}\equiv\boldsymbol{J}_i'.\end{aligned}$$

- For accuracy issues, we iterate on the differences between $\delta\boldsymbol{j}_i^{n+1}$ and $\boldsymbol{J}_i'$.
- For every k_y and k_z mode, the generalized Ohm's law is solved in x direction using finite difference. The equilibrium part is solved by direct matrix inversion. And the nonlinear terms are treated iteratively.

Numerical damping of the whistler wave

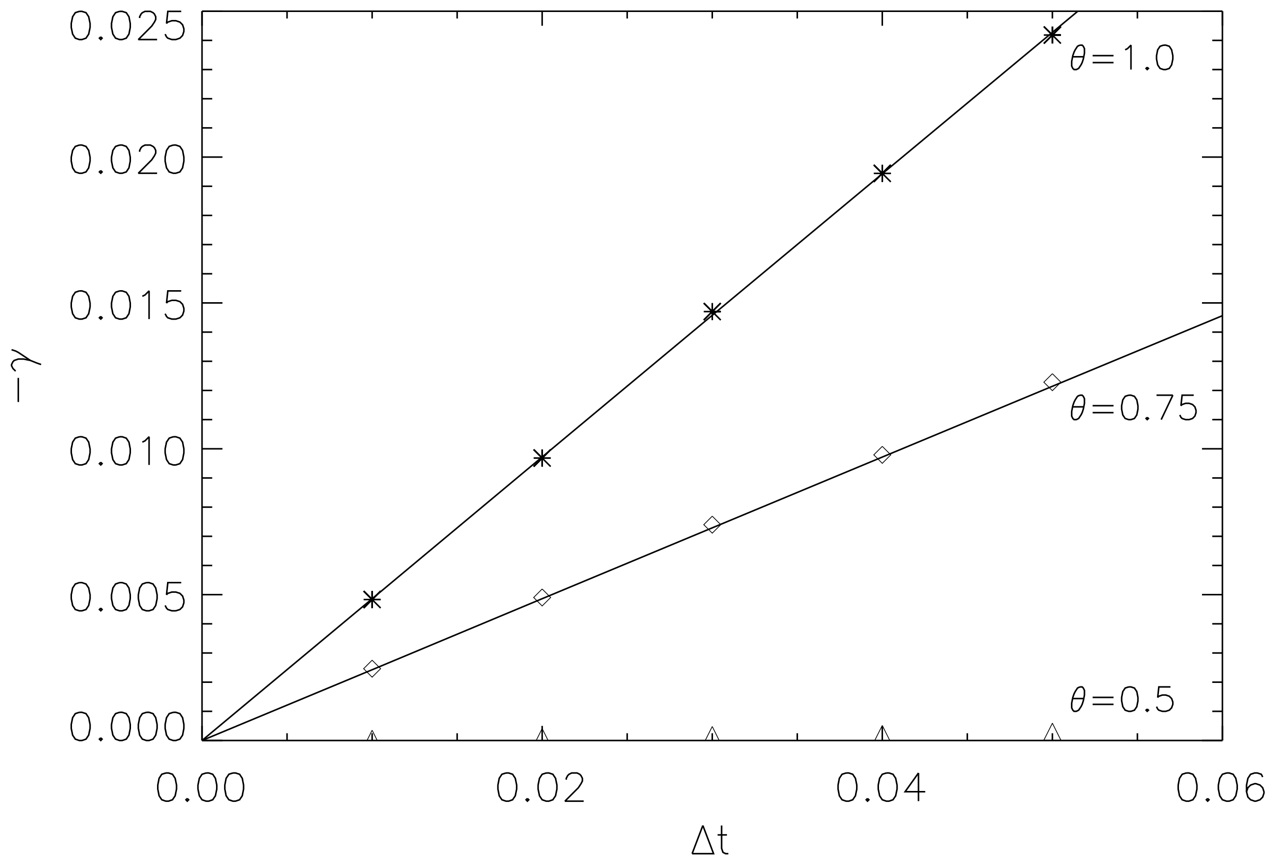

$16 \times 16 \times 32$ grids, 131072 particles, $k_\perp = 0, k_\parallel \rho_i = 0.0628, \beta = 0.004$.

Convergence of the field solver

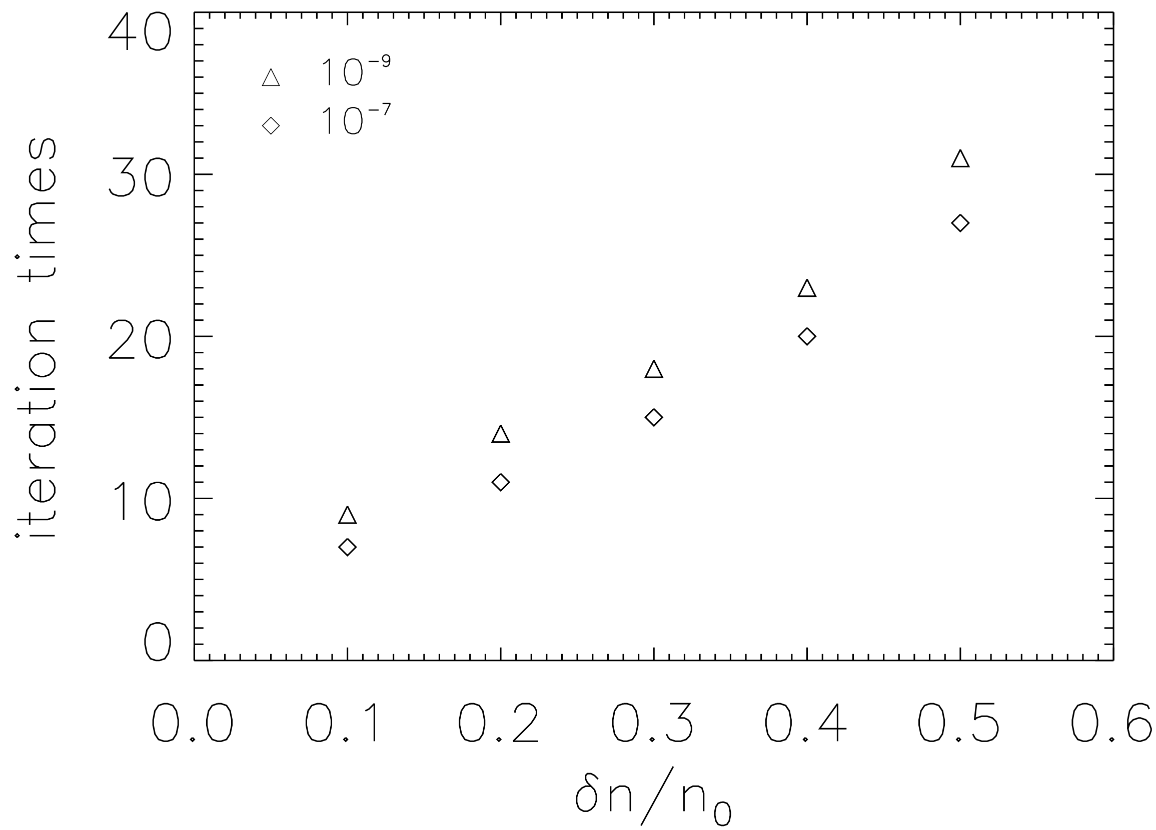

The iteration times needed for field solver to converge to an accuracy order of $\Delta \boldsymbol{E}_x/\boldsymbol{E}_x = 10^{-9}$ (Triangles) and 10^{-7} (Diamonds).

Harris sheet equilibrium

- Zero-order magnetic field $\boldsymbol{B}_0(\boldsymbol{x}) = B_{y0}\tanh(\frac{x}{a})\ \hat{\boldsymbol{y}} + B_G\ \hat{\boldsymbol{z}}$

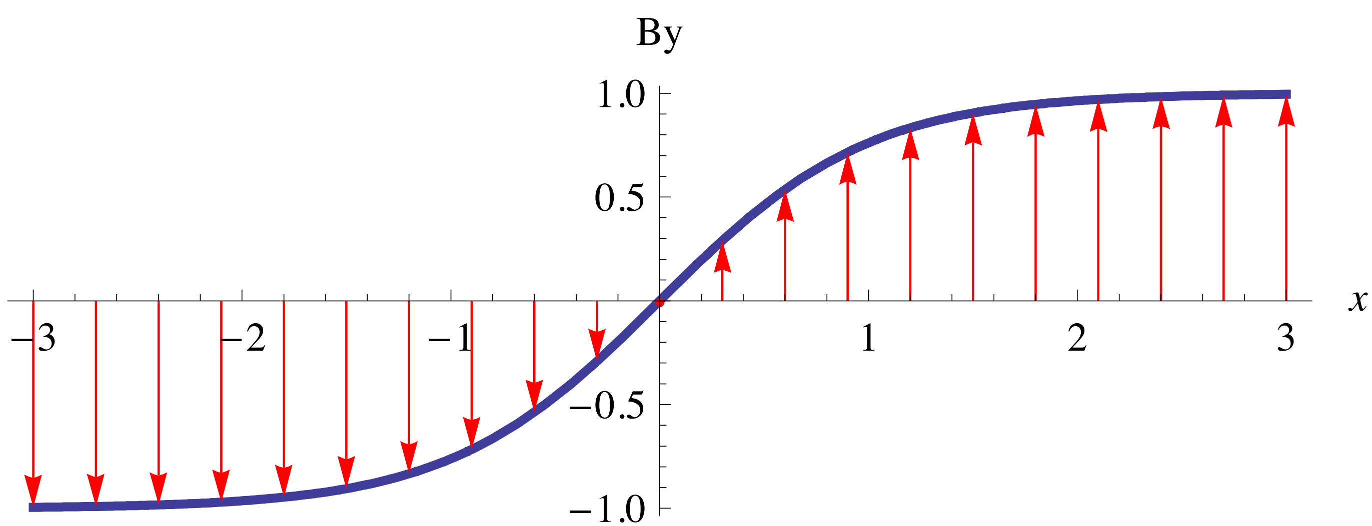

- The equilibrium distribution function is

$$f_{0s} = n_{h0}\ \mathrm{sech}^{\,2}(\frac{x}{a})\left(\frac{2\pi T_s}{m_s}\right)^{-\frac{3}{2}}\exp\left[-\frac{m(v_x^2+v_y^2+(v_z-v_{ds})^2)}{2T_s}\right]$$

$$+n_b\left(\frac{2\pi T_s}{m_s}\right)^{-\frac{3}{2}}\exp\left(-\frac{mv^2}{2T_s}\right),$$

Island and eigenmode structure

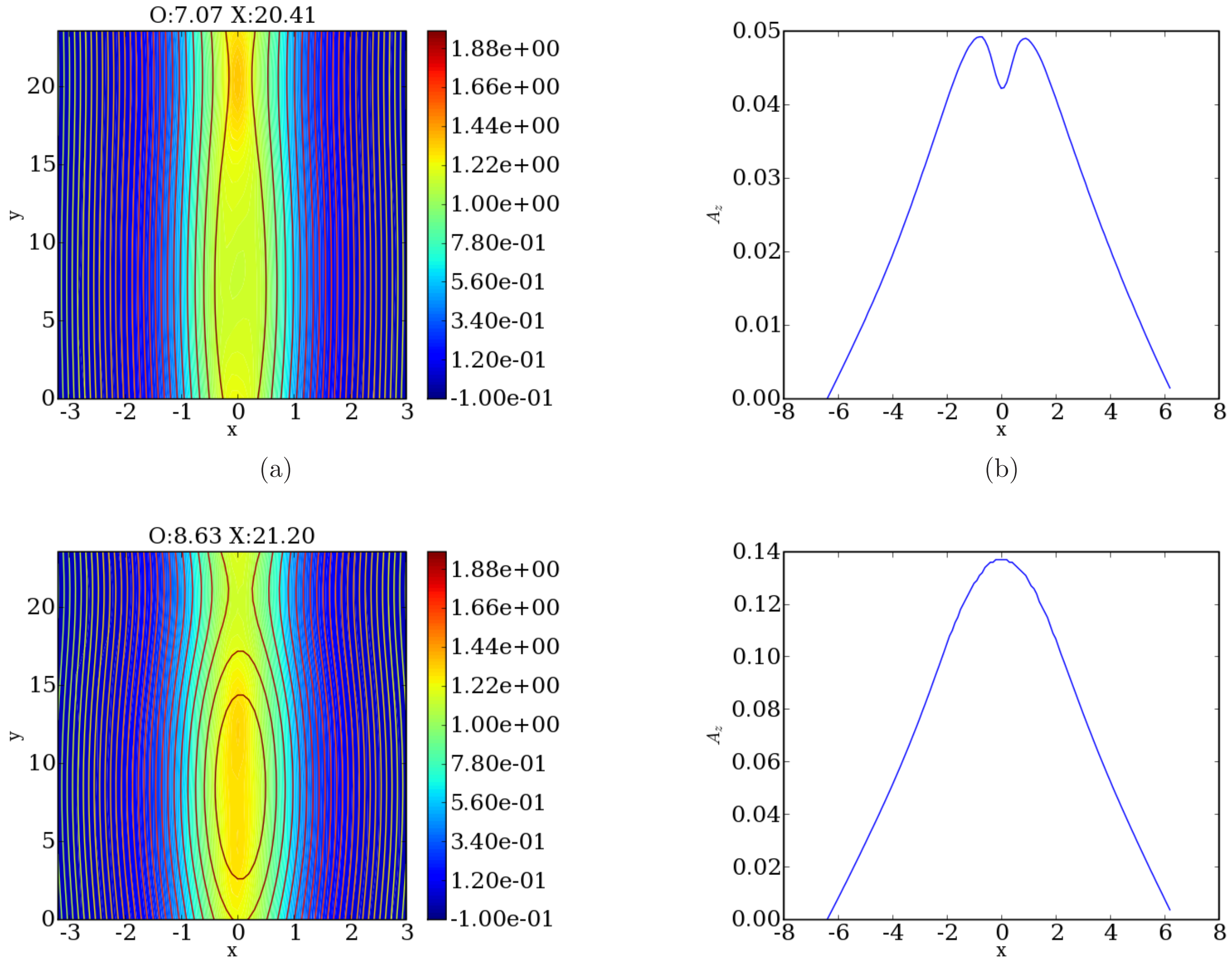

(a) (b) (c) (d)

(a)(b) $t = 233\Omega_i^{-1}$, (c)(d) $t = 495\Omega_i^{-1}$ $128 \times 32 \times 64$ grids, 8388608 particles. $\frac{a}{\rho_i} = 1.0, \beta_e = \frac{\mu_0 n_0 T_e}{B_0^2} = 0.5,$
$\eta \frac{e n_0}{B_0} = 15 \times 10^{-4}, \frac{\boldsymbol{B}_G}{B_0} = 0, \frac{T_i}{T_e} = 1, \frac{l_x}{\rho_i} = 12.8, \frac{l_y}{\rho_i} = 25.12$

The linear growth rate vs η

- Linear Tearing mode theory shows that the growth rate is (scaled)

$$\gamma = \; 0.55\; (\frac{1}{\beta})^{1/5}\; \Delta'^{4/5} \eta^{3/5}\; (k\; B'_{y0})^{2/5}.$$

$$\Delta' = \; \frac{2}{a}(\frac{1}{ka} - ka)\frac{ka - \tanh(l_x/2a)\tanh(kl_x/2)}{ka\tanh(kl_x/2) - \tanh(l_x/2a)}.$$

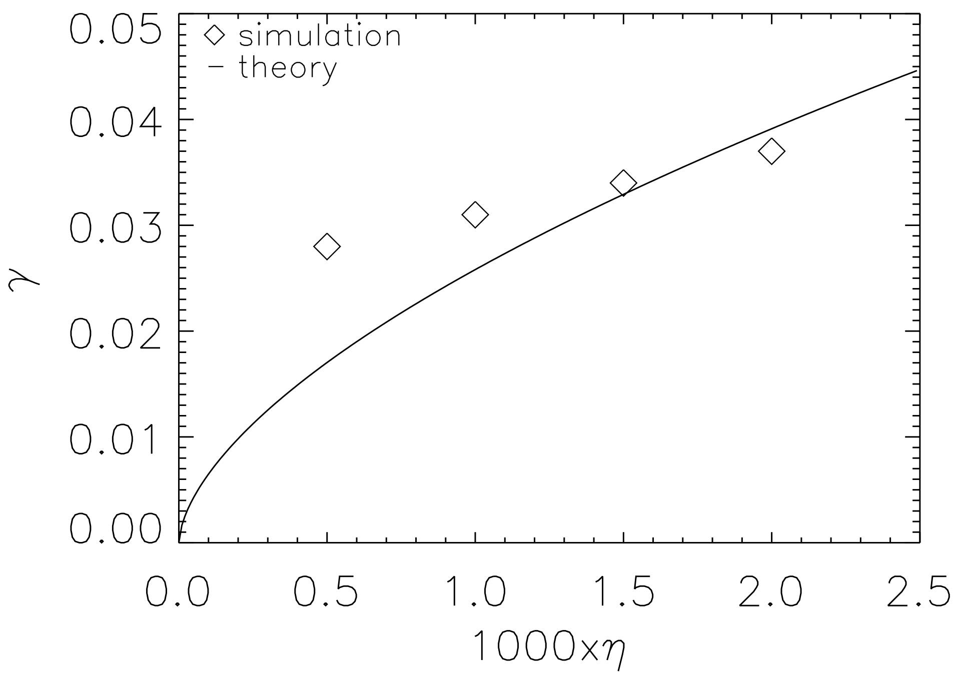

$128 \times 32 \times 64$ grids, 8388608 particles. $\frac{a}{\rho_i} = 1.0, \beta_e = \frac{\mu_0 n_0 T_e}{B_0^2} = 0.5,\ \frac{\boldsymbol{B}_G}{B_0} = 0, \frac{T_i}{T_e} = 1, \frac{l_x}{\rho_i} = 12.8, \frac{l_y}{\rho_i} = 18.84$

The linear growth rate vs k

- Linear Tearing mode theory shows that the growth rate is (scaled)

$$\gamma = 0.55\ (\frac{1}{\beta})^{1/5}\ \Delta'^{4/5}\eta^{3/5}\ (k\ B'_{y0})^{2/5}.$$

$$\Delta' = \frac{2}{a}(\frac{1}{ka} - ka)\frac{ka - \tanh(l_x/2a)\tanh(kl_x/2)}{ka\tanh(kl_x/2) - \tanh(l_x/2a)}.$$

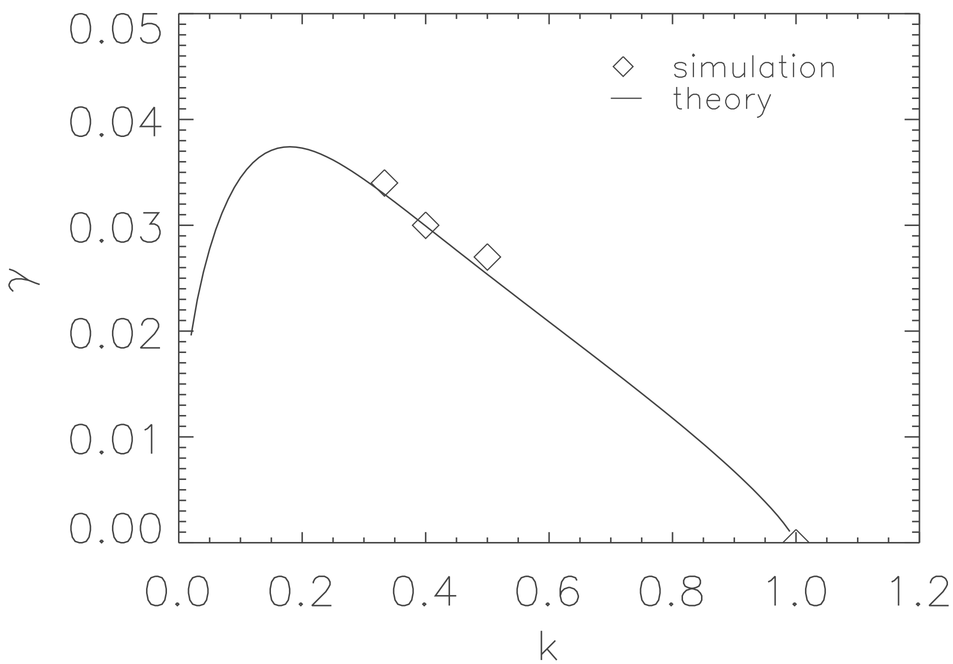

$128 \times 32 \times 64$ grids, 8388608 particles. $\frac{a}{\rho_i} = 1.0, \beta_e = \frac{\mu_0 n_0 T_e}{B_0^2} = 0.5, \frac{\boldsymbol{B}_G}{B_0} = 0, \frac{T_i}{T_e} = 1, \frac{l_x}{\rho_i} = 12.8, \eta = 0.0015$

Full evolution with different Δ'

- Tearing mode evolution with different Δ',

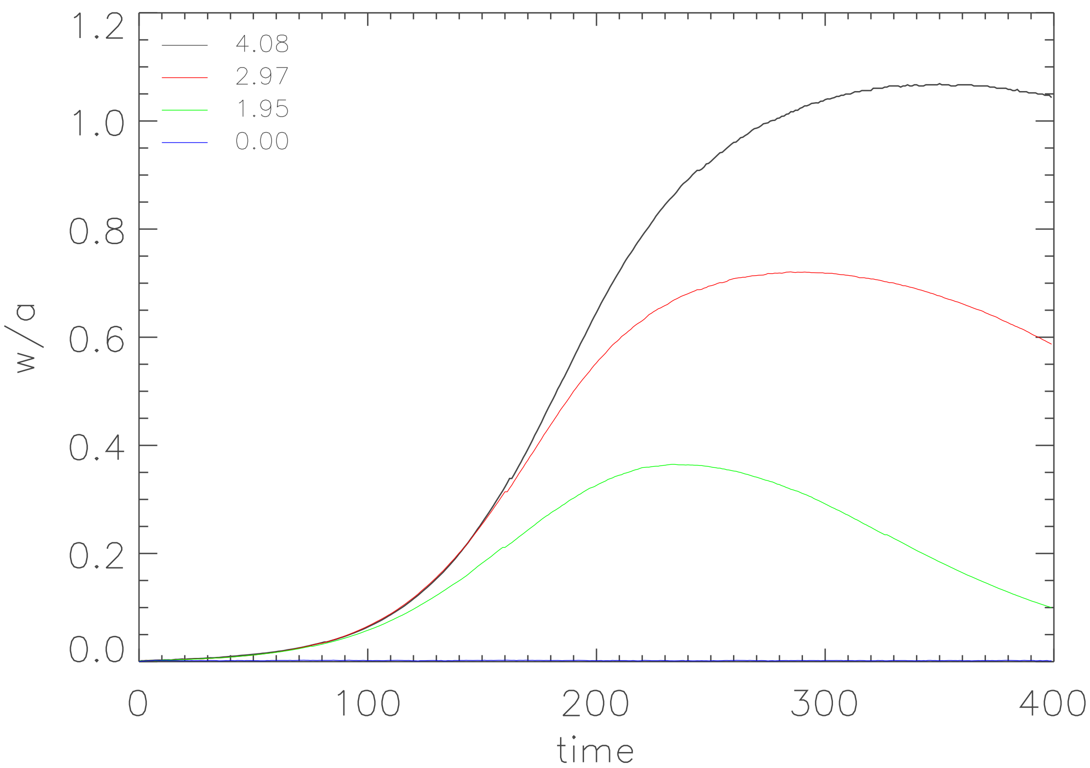

$128 \times 32 \times 64$ grids, 8388608 particles. $\frac{a}{\rho_i} = 1.0, \beta_e = \frac{\mu_0 n_0 T_e}{B_0^2} = 0.5, \frac{\boldsymbol{B}_G}{B_0} = 0, \frac{T_i}{T_e} = 1, \frac{l_x}{\rho_i} = 12.8, \eta = 0.0015$

Rutherford stage

- Island growth can be described by $\frac{dw}{dt} = 1.22\eta(\Delta' - \alpha' w)$, which reduces to the Rutherford equation when w is small ($\alpha' = 0.82$ in this case).

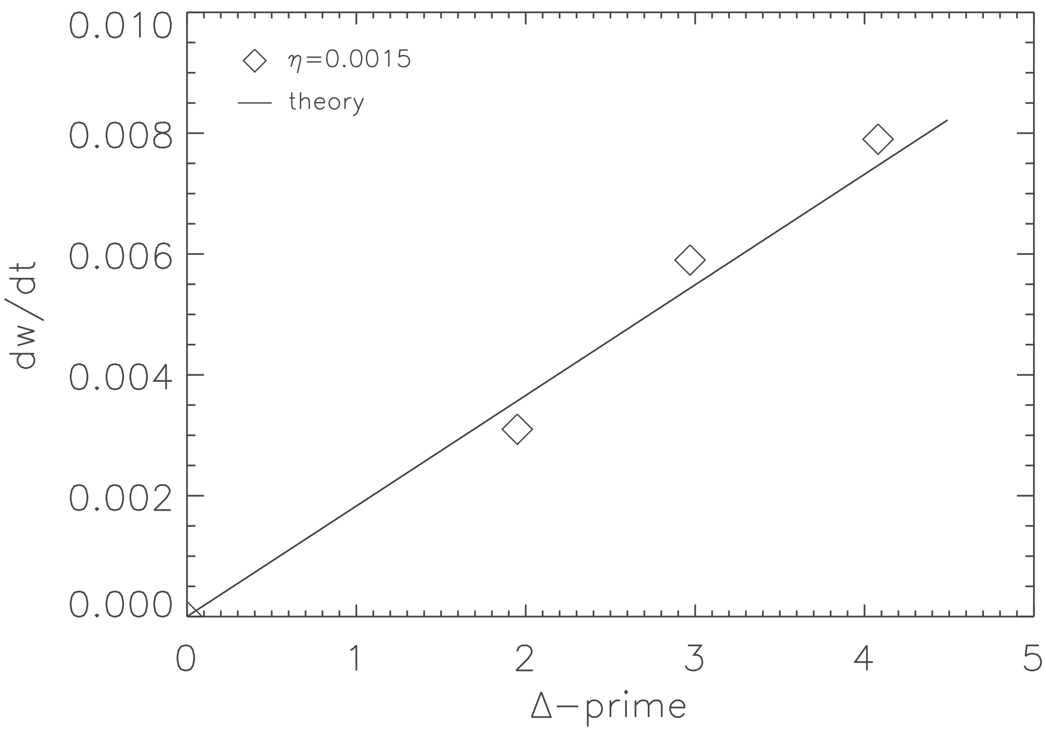

$128 \times 32 \times 64$ grids, 8388608 particles. $\frac{a}{\rho_i} = 1.0, \beta_e = \frac{\mu_0 n_0 T_e}{B_0^2} = 0.5, \frac{\boldsymbol{B}_G}{B_0} = 0, \frac{T_i}{T_e} = 1, \frac{l_x}{\rho_i} = 12.8, \eta = 0.0015$

D. F. Escande and M. Ottaviani, Phys. Lett. A **323**, 278-284(2004)

Island evolution—$\Delta' = 7.875$

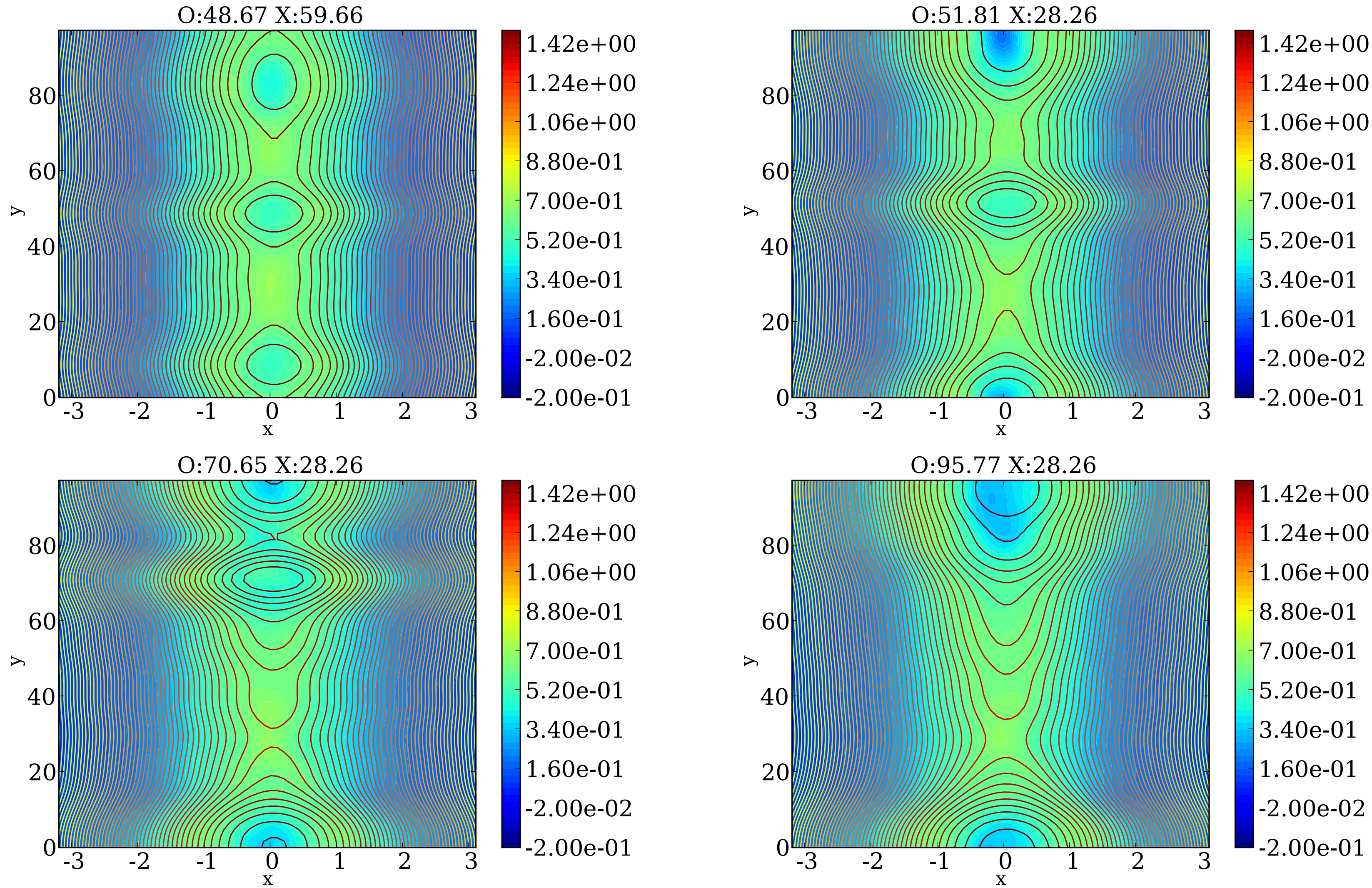

$128 \times 32 \times 64$, 8388608 particles. $\frac{a}{\rho_i} = 2.0$, $\beta_e = \frac{\mu_0 n_0 T_e}{B_0^2} = 0.5$, $\eta \frac{e n_0}{B_0} = 0.0015$, $\frac{\boldsymbol{B}_G}{B_0} = 0$, $\frac{T_i}{T_e} = 1$, $\frac{l_x}{\rho_i} = 12.8$, $\frac{l_y}{\rho_i} = 100.48$

From left to right, top to bottom: $t = 744, 1064, 1532, 1776\ \Omega_i^{-1}$

Saturation

- From the equation $\frac{dw}{dt} = 1.22\eta(\Delta' - \alpha' w)$, the island width at saturation is $w_s = 1.22\Delta'$.

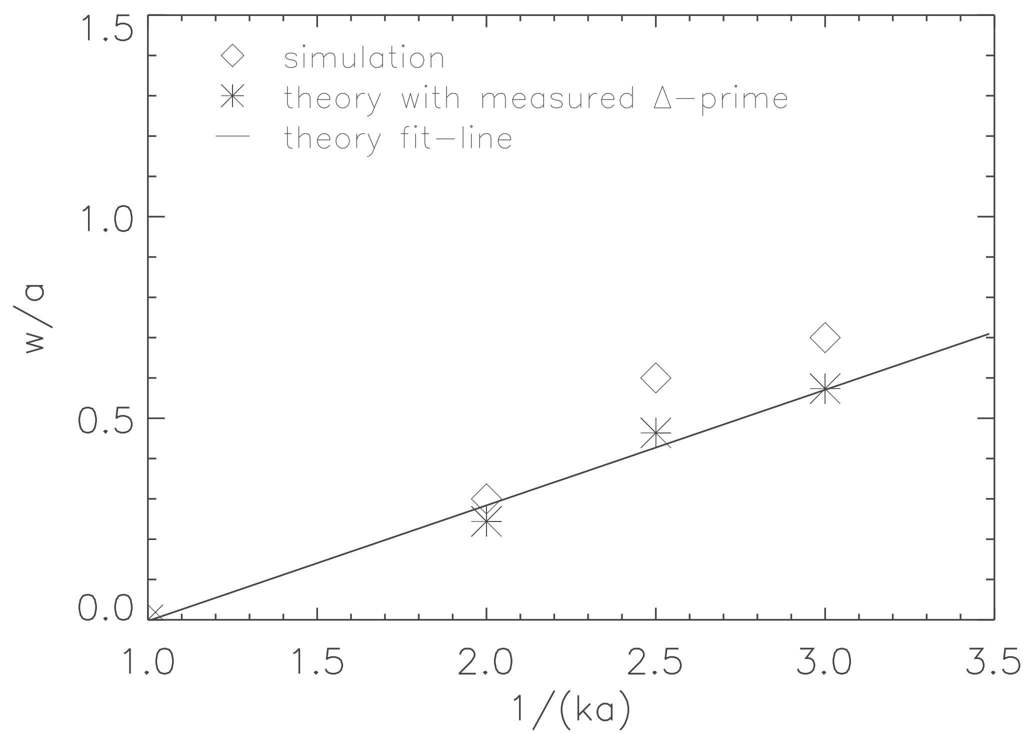

$128 \times 32 \times 64$ grids, 8388608 particles. $\frac{a}{\rho_i} = 1.0, \beta_e = \frac{\mu_0 n_0 T_e}{B_0^2} = 0.5, \frac{\boldsymbol{B}_G}{B_0} = 0, \frac{T_i}{T_e} = 1, \frac{l_x}{\rho_i} = 12.8, \eta = 0.0015$

Measurement of the Δ'

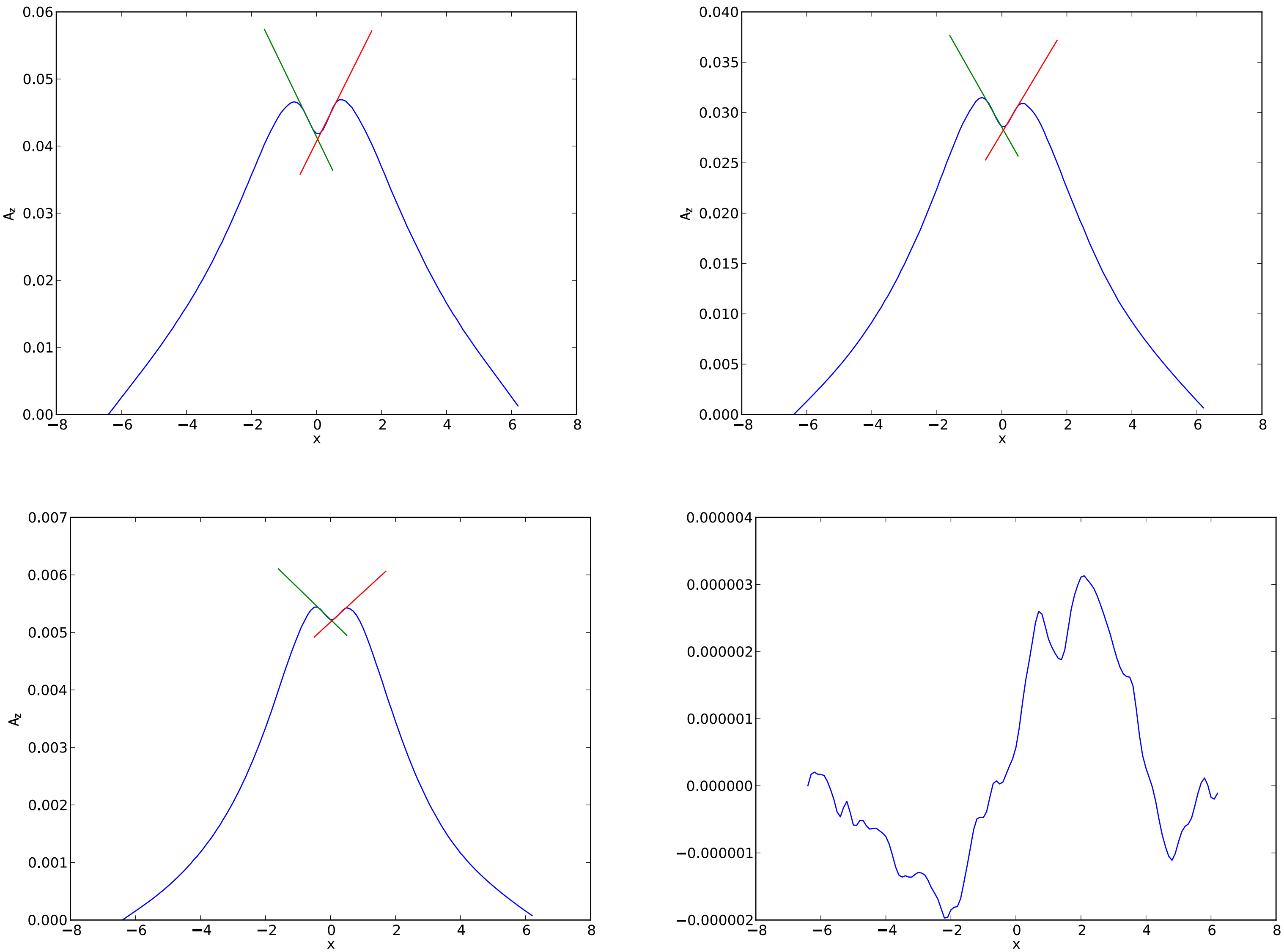

$128 \times 32 \times 64$ grids, 8388608 particles. $\frac{a}{\rho_i} = 1.0, \beta_e = \frac{\mu_0 n_0 T_e}{B_0^2} = 0.5, \frac{\boldsymbol{B}_G}{B_0} = 0, \frac{T_i}{T_e} = 1, \frac{l_x}{\rho_i} = 12.8, \eta = 0.0015$

Summary

1. We have implemented a second-order accurate implicit algorithm with Lorentz force ions and isothermal fluid electrons which is
   - Quasi-neutral and fully electromagnetic.
   - Suitable for MHD scale plasmas.

2. Demonstrated 3-D slab simulation for Alfvèn waves, whistler wave, and the ion acoustic wave. Showed that the time-centered second order scheme brings no numerical damping through whistler waves studies.

3. The full evolution of resistive tearing mode is investigated with Harris sheet equilibrium.

4. Results showing formation of multiple islands and coelescence during large Δ' tearing mode evolution. Further study is needed to better understand the nonlinear dynamics.